ELSEVIER

Journal of Nuclear Materials 283–287 (2000) 483–487

journal of nuclear materials

www.elsevier.nl/locate/jnucmat

Tensile properties and microstructure of 590 MeV proton-irradiated pure Fe and a Fe–Cr alloy

M.I. Luppo [1], C. Bailat, R. Schäublin, M. Victoria *

Centre of Research in Plasma Physics, Swiss Federal Institute of Technology- Lausanne, Fusion Technology Materials Division, 5232 Villigen–PSI, Switzerland

Abstract

Polycrystalline pure Fe and Fe–12Cr alloy have been proton-irradiated to doses of 10^{-3}–3×10^{-1} dpa at room temperature and 523 K. Samples were mechanically tested in tension and transmission electron microscopy (TEM) was performed on the as-irradiated material as well as on the irradiated and deformed material. At room temperature, pure Fe presents an initial yield point, that increases with the dose, followed by a yield region, indicative of a localized deformation mode. The Fe–12Cr alloy shows the same behavior, but the irradiation amplifies the effects previously mentioned. No yield point or yield region appears after irradiation at 523 K. TEM observations of the irradiated material showed a high density of small defect clusters which increases with the dose. Defect-free channels are observed in Fe–12Cr irradiated and deformed at room temperature. Results of the present investigation are compared with neutron irradiation of similar materials.

1. Introduction

Ferritic–martensitic steels are attractive as candidate structural materials in a fusion reactor because of their high resistance to swelling up to damage doses of 200 dpa [1]. Furthermore, high Cr ferritic alloys have excellent resistance to helium embrittlement and to irradiation creep [2].

Unfortunately, most of these steels exhibit low-temperature irradiation-induced embrittlement, that imposes a severe restriction on their reactor applications at temperatures below 673 K [3]. However, the behavior of ferritic–martensitic alloys depends on composition, processing and the resulting microstructures, so by optimizing these parameters, as is the case in the low-activation versions of these steels, very low ductile–brittle transition temperatures can be obtained [4,5]. In particular, the 9% Cr composition has been shown to be less susceptible to radiation hardening [6]. In ferrite, the radiation hardening increases with Cr content [2,7], while the ductile–brittle transition temperature is reduced to 160 K at 15% Cr [2].

The current investigation is part of a program in which the differences in microstructure and radiation induced hardening between pure Fe, Fe–12% Cr ferrite and Fe–12% Cr–0.2% C martensite are compared. In a previous publication [8] the behavior of pure Fe irradiated with 590 MeV protons was compared to that after neutron irradiation. In the present study, the irradiation induced defect structure and its effect on the mechanical properties in a polycrystalline iron and the ferritic Fe–12Cr alloy is investigated.

2. Experimental procedure

The materials used in the present research were a polycrystalline pure Fe (99.95%; $C < 0.01$ ppm) and a ferritic Fe–12Cr alloy (11.73% Cr, 0.011% C).

Pure Fe was heat treated at 923 K for 60 min to obtain a recrystallized grain size of about 30 μm [8]. Polycrystalline Fe–12Cr was heat treated at 970 K for 20

* Corresponding author. Tel.: +41-56 99 20 63; fax: +41-56 99 45 29.

E-mail addresses: maria.luppo@psi.ch (M.I. Luppo), max.victoria@psi.ch (M. Victoria).

[1] Tel.: +41-56 310 4538; fax: +41-56 310 4529. On leave from Materials Department, Comisión Nacional de Energía Atómica, Argentine.

0022-3115/00/$ - see front matter
PII: S0022-3115(00)00370-6

min to recrystallize the material to a final grain size of about 60 μm.

Flat microtensile specimens (gauge length: 5.5 mm, thickness: 2.5 mm) are used for tensile tests which were spark cut from foils. Tensile tests were performed in a Schenck machine at a strain rate of 6×10^{-5} s^{-1}. Tests at room temperature were performed in air and tests at 523 K were performed in vacuum.

Irradiations were performed on the tensile test specimens in the PIREX [9] facility which uses the 590 MeV proton beam of the accelerator at the Paul Scherrer Institute in Switzerland. The damage rate is approximately 1.3×10^{-6} dpa s^{-1}. The irradiation matrix for pure Fe included doses from 10^{-3} to 0.3 dpa at 293 and 523 K. The Fe–12Cr alloy was irradiated at 293 and 523 K up to a dose of 0.2 dpa. The actual dose was determined by using the γ-line emitted by the ^{54}Mn radioisotope produced by the proton irradiation.

Specimens suitable for transmission electron microscopy (TEM) were cut from the irradiated tensile samples and were prepared as described in Ref. [10]. The observations were performed in a JEOL 2010 operating at 200 keV. The defect microstructure was observed mainly under weak-beam dark-field (g, $4g$) imaging conditions using diffraction vectors $\boldsymbol{g}$ of the $\langle 1\,1\,0\rangle$ type.

3. Results

3.1. Tensile tests

Fig. 1 shows the tensile behavior of Fe and Fe–12Cr tested at room temperature. In unirradiated Fe, a yield point is followed by a yield region induced by the propagation of Lüders bands, usually associated with small amounts of interstitial impurities (C,N). In the irradiated material, radiation hardening is observed, and the tensile curves show an initial yield point followed by a yield region up to a dose of 0.33 dpa. The lower yield stress increases while the work hardening and the total elongation decrease with dose. At higher doses, although the yield stress continues to increase, the yield point disappears and little or no work hardening is observed.

A yield stress increase and a reduction in the total elongation is also observed in the Fe–12Cr specimen irradiated to a dose level of 0.2 dpa, but no yield point or Lüders band propagation is observed in the unirradiated specimen. The yield region is present in the irradiated sample, but due to a failure of the recording, the initial part of the tensile curve shown was obtained from point data rather than from the continuous trace of the load–extension curve. The radiation hardening measured by the difference of yield strength between the irradiated and unirradiated samples is higher for the Fe–12Cr alloy (153 MPa) than for the pure Fe (138 MPa) at a comparable dose.

In the stress–strain curves of Fe and Fe–12Cr irradiated and tested at 523 K, Fig. 2, there is no yield point or yield region in all cases. The behavior of Fe is quite different at this temperature: both the ultimate tensile strength and the work hardening decrease with increasing dose. There is a small increase in yield strength (∼45 MPa) with respect to the unirradiated material, but the yield stress itself (YS ∼ 145 MPa) does not change with increasing dose, up to 3.4×10^{-2} dpa.

The Fe–Cr alloy, irradiated to 0.2 dpa at 523 K, shows radiation hardening and a total elongation decrease. The increase in yield strength is in fact higher (178 MPa) than that found at room temperature.

3.2. TEM observations

(i) *The defect microstructure*: Fig. 3(a) shows the defect microstructure produced by 590 MeV protons in Fe.

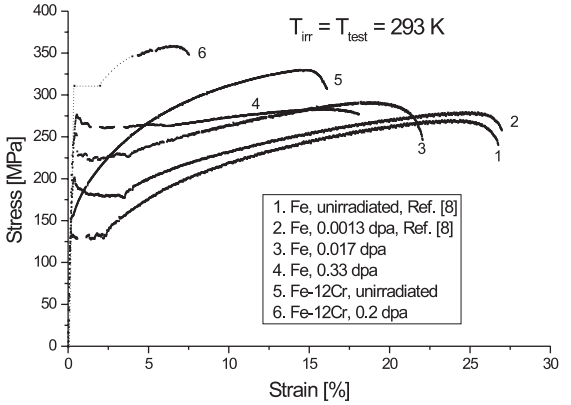

Fig. 1. Tensile stress–strain curves of unirradiated and proton-irradiated specimens of Fe and Fe–12Cr alloy at room temperature.

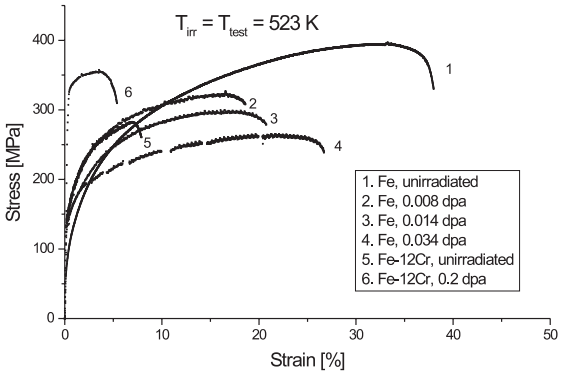

Fig. 2. Tensile stress–strain curves of unirradiated and proton-irradiated specimens of Fe and Fe–12Cr alloy at 523 K.

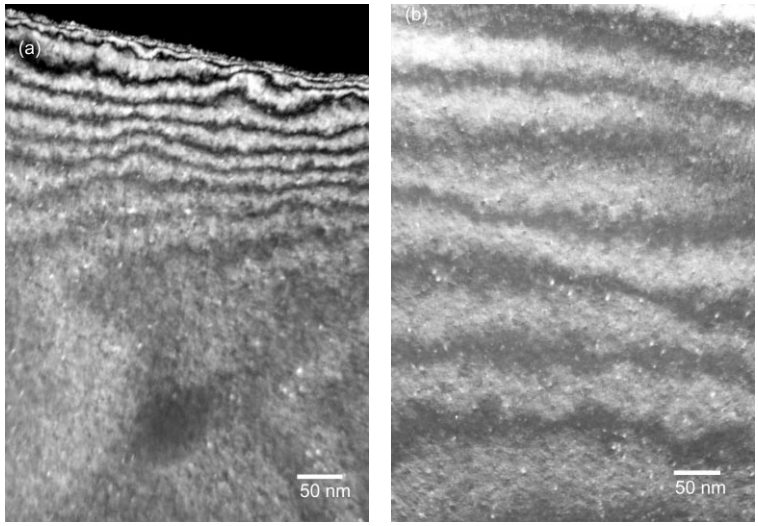

Fig. 3. Defect clusters in: (a) Fe proton-irradiated at room temperature to a dose of 0.33 dpa. (b) Fe–12Cr proton-irradiated at room temperature to a dose of 0.2 dpa. Weak-beam (g,4g), $g = \langle 1\,1\,0\rangle$.

The microstructure consists of small defect clusters, though to be interstitial in character. The structure obtained in the irradiated Fe–12Cr alloy is comparable, Fig. 3(b).

As shown in Fig. 4, the cluster density of pure irradiated Fe at room temperature and at 523 K increases with the dose, but at a slightly different rate. Results of the present work are compared in the same figure with those obtained for the same material after neutron irradiation [11].

At room temperature, the average defect-size is about 3.3 nm and this value is constant with dose up to 3.4×10^{-2} dpa. Somewhat higher mean sizes ($\sim$4.8 nm) are found after irradiation at 523 K.

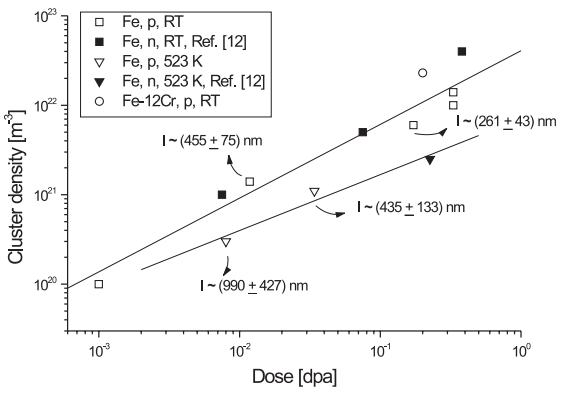

Fig. 4. Dose dependence of the defect density in Fe and Fe–12Cr alloy irradiated with protons (p) and neutrons (n). l is the mean obstacle distance.

(ii) *Deformation mode*: In Fe, it is well established that the deformation mode in room temperature deformation is dislocation channeling [11]. As shown in Fig. 5 it is also observed after deformation of the Fe–12Cr alloy. The channel width is typically 60–100 nm and it develops on $\langle 1\,1\,0\rangle$ type slip planes.

4. Discussion

In the case of irradiated Fe, the presence of a yield point can be explained by the locking of the initial dislocation structure by the loops produced by irradiation [12,13]. The yield region that follows the yield point has been shown to be associated with the localization of the strain due to the propagation of dislocation channels in Cu [14], Pd [15] and Fe [11]. The work hardening response after this yield region follows a Hollomon law ($\sigma_p = K\varepsilon_p^n$) behavior, where the work hardening exponent n decreases with dose, as shown in Fig. 6. Similar results are found in [7]. At a dose of 0.33 dpa the deformation seems to be controlled only by the propagation of channels, with a strong reduction in the ductility.

The radiation hardening of Fe at room temperature by the protons increases with dose as shown in Fig. 7, where two other sets of data obtained after neutron irradiations are also included. The response is quite different: the results of Hammad et al. [7] indicate a $(\text{dose})^{1/2}$ behavior, while that of Singh et al. [11], which were obtained in the same material as the present investigation, follow a $(\text{dose})^{1/3}$ regime. The hardening response to protons is much lower, fitting approximately a $(\text{dose})^{1/5}$ response. In these last two cases, the

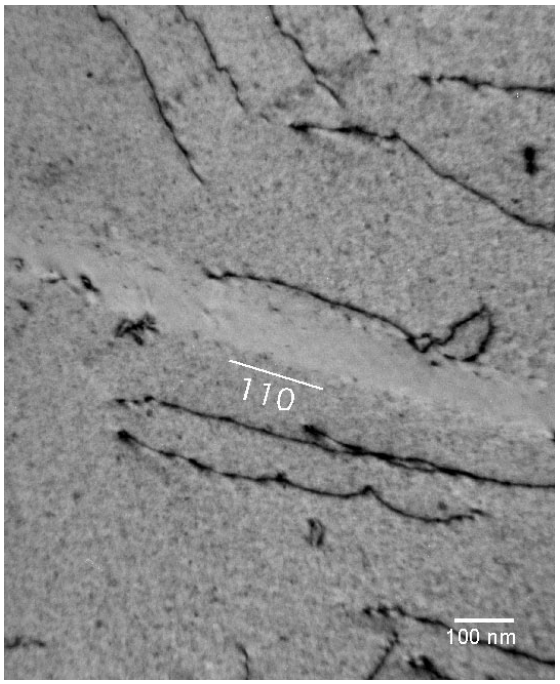

Fig. 5. Defect-free channel in the deformed proton-irradiated Fe–12Cr alloy at room temperature. Imaging conditions: $g = \langle 1\,1\,0\rangle$, $z = \langle 1\,1\,1\rangle$.

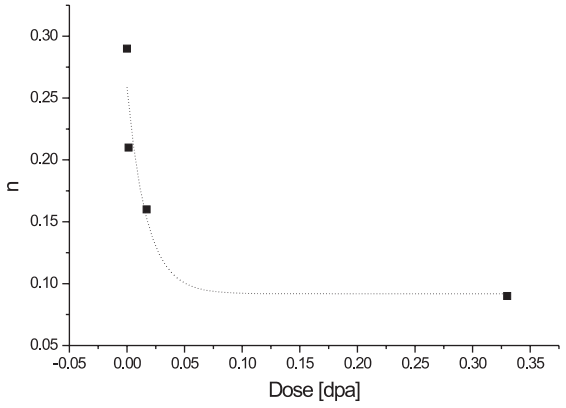

Fig. 6. Strain-hardening coefficient vs dose of unirradiated and irradiated specimens of Fe at room temperature.

irradiation induced defect clusters have comparable number densities, see Fig. 4, but the mean size is somewhat larger in the neutron irradiation case, 5 nm compared to 3 nm in the proton case at 0.33 dpa. In analyzing in detail the three sets of data, the origin of these differences seems to be originated in the different strain rates used: 10^{-3} s^{-1} for both neutron-irradiated cases and 6×10^{-5} s^{-1} in the present investigation. The $\Delta\sigma$ values are systematically higher at the higher strain rates.

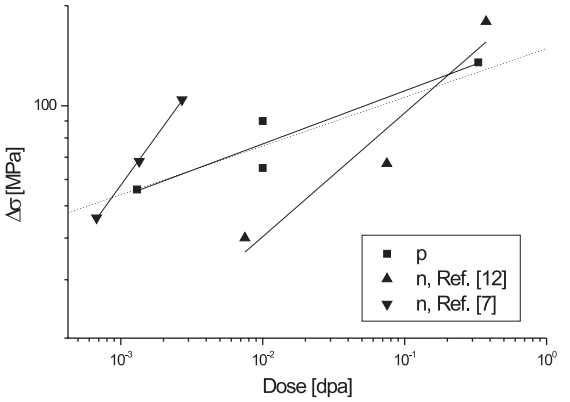

Fig. 7. Dose dependence of the increase in yield stress in Fe irradiated with protons (p) and neutrons (n) at room temperature.

After irradiation and deformation at 523 K, very little hardening is measured in Fe, and the work hardening decreases with dose, up to a dose of 0.034 dpa. In Fig. 4, the mean obstacle distances, $l = (Nd)^{-1/2}$ where N is the number density of defects and d their mean size, are indicated showing that there is a coarsening of the defect cluster microstructure. Due to the low number densities measured at the lower dose, the errors are large, as indicated, and do not clearly define an increase in obstacle distribution that the dislocations have to surmount.

The Fe–12Cr alloy shows radiation hardening at both irradiation and test temperatures, the hardening being stronger than in Fe and more important at the higher irradiation temperature (178 MPa as compared to 153 MPa at room temperature). The presence of a yield region in the deformation at room temperature is indicative of a localized deformation mode, which is typical in this temperature regime when dislocation channeling is operating. Fig. 5 confirms the presence of dislocation channels in the deformed Fe–12Cr alloy.

5. Conclusions

From the tensile tests and TEM observations in a pure Fe and a Fe–12Cr alloy proton-irradiated at room temperature and 523 K, it can be concluded that:

(i) At room temperature:

- All the irradiated materials show an initial yield point attributed to the locking of the initial dislocation structure by the defects produced by irradiation. The increase in the yield point with the dose is related to the increase in the defect density.
- The yield point is followed by a yield region associated with the localization of the deformation due to the propagation of dislocation channels. This is con-

firmed by the presence of defect-free channels in the Fe–12Cr alloy.
- The work hardening presented a decrease with the dose and follows a Hollomon type law.

(ii) At 523 K:
- There is no yield point or yield region, indicating a change in the deformation mode.
- The cluster density increases at a slower rate with dose when compared with the behavior at room temperature.

Acknowledgements

The financial aid of the European fusion materials program and of the Swiss Research Council is gratefully acknowledged. One of the authors (M.I.L.) wishes to express her gratitude to the Fundación Antorchas for the travel funds received.

References

[1] D.S. Gelles, J. Nucl. Mater. 225 (1995) 163.
[2] K. Suganuma, H. Kayano, S. Yajima, J. Nucl. Mater. 105 (1982) 23.
[3] S.I. Porollo, A.M. Dvoriashin, A.N. Vorobyev, Y.V. Konobeev, J. Nucl, Mater. 256 (1998) 247.
[4] E.A. Little, J. Nucl. Mater. 206 (1993) 324.
[5] M. Victoria, E. Batawi, Ch. Briguet, D. Gavillet, P. Marmy, J. Peters, F. Rezai Aria, in: D.S. Gelles, R.K. Nanstad, A.S. Kumar, E.A. Little, (Eds.), Effects of Radiation on Materials: 17th International Symposium, ASTM STP 1270, (1996) 721.
[6] R.I. Klueh, J. Nucl. Mater. 179–181 (1991) 728.
[7] F.H. Hammad, M.K. Matta, K.E. Mohammed, J. Nucl. Mater. 108&109 (1982) 428.
[8] Y. Chen, P. Spätig, M. Victoria, J. Nucl. Mater. 271&272 (1999) 128.
[9] P. Marmy, M. Daum, D. Gavillet, S. Green, W.V. Green, F. Hegedus, S. Proennecke, U. Rohrer, U. Stiefel, M. Victoria, Nucl. Instrum. and Meth. B 47 (1990) 37.
[10] R. Schaüblin, M. Victoria, these Proceedings, p. 339.
[11] B.N. Singh, A. Horsewell, P. Toft, J. Nucl. Mater. 271–272 (1999) 97.
[12] B.N. Singh, A.J.E. Foreman, H. Trinkaus, J. Nucl. Mater. 249 (1997) 103.
[13] M. Victoria, N. Baluc, C. Bailat, Y. Dai, M.I. Luppo, R. Schaublin, B.N. Singh, J. Nucl. Mater. 276 (2000) 114.
[14] Y. Dai, M. Victoria, Mater. Res. Symp. Proc. 439 (1996) 319.
[15] N. Baluc, Y. Dai, M. Victoria, Mater. Res. Symp. Proc. 540 (1999).